

# Effect of hyperon-hyperon interaction on bulk viscosity and r-mode instability in neutron stars

Debarati Chatterjee and Debades Bandyopadhyay

*Saha Institute of Nuclear Physics, 1/AF Bidhannagar, Kolkata-700064, India*

## Abstract

We investigate the effect of hyperon matter including hyperon-hyperon interaction on bulk viscosity. Equations of state are constructed within the framework of a relativistic field theoretical model where baryon-baryon interaction is mediated by the exchange of scalar and vector mesons. Hyperon-hyperon interaction is also taken into account by the exchange of two strange mesons. This interaction results in a smaller maximum mass neutron star compared with the case without the interaction. The coefficient of bulk viscosity due to the non-leptonic weak process is determined by these equations of state. The interacting hyperon matter reduces the bulk viscosity coefficient in a neutron star interior compared with the no interaction case. The r-mode instability is more effectively suppressed in hyperon-hyperon interaction case than that without the interaction.

PACS numbers:

## I. INTRODUCTION

Neutron stars may undergo various instabilities which are associated with unstable modes of oscillation [1]. To understand oscillatory modes of a neutron star one has to study its stability properties. Each physical restoring force acting on a fluid element leads to a new family of oscillatory modes. Pulsation modes of neutron stars are classified according to different restoring forces. Here we are interested in Coriolis restored inertial r-modes. It was shown that r-modes were subject to Chandrasekhar-Friedman-Schutz gravitational radiation instability in rapidly rotating neutron stars [1, 2, 3, 4, 5, 6]. This instability may play an important role in regulating spins of young neutron stars as well as old, accreting neutron stars in low mass x-ray binaries (LMXBs) and provides a plausible explanation for the absence of very fast rotating neutron stars in nature. This finds support from the study of eleven nuclear-powered millisecond pulsars whose spin frequencies are known from burst oscillations has shown that the spin distribution has an upper limit at 730 Hz [7, 8]. Recently observed fastest rotating neutron star is a radio pulsar with a spin frequency 716 Hz [9]. The r-mode instability could be a possible source for gravitational radiation [1, 10]. And, the detection of gravitational emission due to r-mode instability may shed light on the interior composition of a neutron star.

It was argued that the r-mode instability could be effectively suppressed by bulk viscosity due to exotic matter in neutron star interior. Neutron star matter encompasses a wide range of densities, from the density of iron nucleus at the surface of the star to several times normal nuclear matter density in the core. Since the chemical potentials of nucleons and leptons increase rapidly with density in the interior of neutron stars, different kinds of exotic matter with large strangeness fraction such as, hyperon matter, Bose-Einstein condensed matter of antikaons and quark matter may appear there. The coefficient of bulk viscosity due to non-leptonic weak processes involving hyperons was calculated by several authors [11, 12, 13, 14, 15]. It was noted that when the gravitational-radiation growth time scale was longer than the damping time scale due to hyperon bulk viscosity, the r-mode instability would be completely suppressed. Actually, a window of instability was found in the calculations of Ref.[13, 15]. Also, the impact of bulk viscosity due to unpaired and paired quark matter on the r-mode instability had been investigated extensively [15, 16, 17, 18].

Earlier studies showed that hyperons might appear in neutron star matter around 2-3

normal nuclear matter density [19, 20]. It was also noted that  $\Lambda$  hyperons appeared first in the system followed by  $\Xi$  hyperons [20]. On the other hand  $\Sigma$  hyperons were excluded from the system because of a repulsive  $\Sigma$  hyperon potential depth at normal nuclear matter density [21]. Also, hyperon-hyperon interaction becomes important because the matter is hyperon-rich at high density regime. This interaction was accounted by the exchange of two strange mesons,  $f_0$  (975) (denoted hereafter as  $\sigma^*$ ) and  $\phi$  (1020) [22, 23]. It was found that the competition between attractive  $\sigma^*$  and repulsive  $\phi$  fields made the overall equation of state stiffer at higher densities [23]. In previous investigations of hyperon bulk viscosity,  $\Sigma$  hyperons appeared before  $\Lambda$  hyperons because an attractive  $\Sigma$  hyperon potential at normal nuclear matter density was considered. Those calculations also did not include hyperon-hyperon interaction.

In this paper, we investigate the effect of hyperon-hyperon interaction on bulk viscosity coefficient, the corresponding damping timescale and the r-mode stability. Further, we use recent experimental data of hypernuclei to determine hyperon-scalar meson couplings in this calculation. This paper is organized in the following way. In Sec. II, we describe the model to calculate equation of state (EoS), bulk viscosity coefficient and the corresponding timescale. Parameters and results of our calculation are discussed in Sec. III. We summarise and conclude in Sec. IV.

## II. FORMALISM

We adopt a relativistic field theoretical model to describe the  $\beta$ -equilibrated and charge neutral hadronic matter. The constituents of matter are  $n, p, \Lambda, \Sigma^+, \Sigma^-, \Sigma^0, \Xi^-, \Xi^0$  of the baryon octet and electrons and muons. In this model, baryon-baryon interaction is mediated by the exchange of scalar and vector mesons and for hyperon-hyperon interaction, two additional mesons - scalar  $\sigma^*$  and vector  $\phi$  [22, 23] are incorporated. Therefore the Lagrangian density for the hadronic phase is given by

$$\begin{aligned}
\mathcal{L}_B = & \sum_B \bar{\Psi}_B (i\gamma_\mu \partial^\mu - m_B + g_{\sigma B} \sigma - g_{\omega B} \gamma_\mu \omega^\mu - g_{\rho B} \gamma_\mu \mathbf{t}_B \cdot \boldsymbol{\rho}^\mu) \Psi_B \\
& + \frac{1}{2} (\partial_\mu \sigma \partial^\mu \sigma - m_\sigma^2 \sigma^2) - U(\sigma) \\
& - \frac{1}{4} \omega_{\mu\nu} \omega^{\mu\nu} + \frac{1}{2} m_\omega^2 \omega_\mu \omega^\mu - \frac{1}{4} \boldsymbol{\rho}_{\mu\nu} \cdot \boldsymbol{\rho}^{\mu\nu} + \frac{1}{2} m_\rho^2 \boldsymbol{\rho}_\mu \cdot \boldsymbol{\rho}^\mu + \mathcal{L}_{YY} . \tag{1}
\end{aligned}$$

The isospin multiplets for baryons  $B = N, \Lambda, \Sigma$  and  $\Xi$  are represented by the Dirac spinor  $\Psi_B$  with vacuum baryon mass  $m_B$ , and isospin operator  $t_B$  and  $\omega_{\mu\nu}$  and  $\rho_{\mu\nu}$  are field strength tensors. The scalar self-interaction term [24] is

$$U(\sigma) = \frac{1}{3}g_2\sigma^3 + \frac{1}{4}g_3\sigma^4. \quad (2)$$

The Lagrangian density for hyperon-hyperon interaction ( $\mathcal{L}_{YY}$ ) is given by

$$\begin{aligned} \mathcal{L}_{YY} = & \sum_B \bar{\Psi}_B (g_{\sigma^*B}\sigma^* - g_{\phi B}\gamma_\mu\phi^\mu) \Psi_B \\ & + \frac{1}{2} (\partial_\mu\sigma^*\partial^\mu\sigma^* - m_{\sigma^*}^2\sigma^{*2}) - \frac{1}{4}\phi_{\mu\nu}\phi^{\mu\nu} + \frac{1}{2}m_\phi^2\phi_\mu\phi^\mu. \end{aligned} \quad (3)$$

We perform this calculation in the mean field approximation [25]. The mean values for corresponding meson fields are denoted by  $\sigma, \sigma^*, \omega_0, \rho_{03}$  and  $\phi_0$ . Therefore, we replace meson fields with their expectation values and meson field equations become

$$m_\sigma^2\sigma = -\frac{\partial U}{\partial\sigma} + \sum_B g_{\sigma B}n_B^s, \quad (4)$$

$$m_{\sigma^*}^2\sigma^* = \sum_B g_{\sigma^*B}n_B^s, \quad (5)$$

$$m_\omega^2\omega_0 = \sum_B g_{\omega B}n_B, \quad (6)$$

$$m_\phi^2\phi_0 = \sum_B g_{\phi B}n_B, \quad (7)$$

$$m_\rho^2\rho_{03} = \sum_B g_{\rho B}I_{3B}n_B. \quad (8)$$

The scalar density and baryon number density are

$$n_B^S = \frac{2J_B + 1}{2\pi^2} \int_0^{k_{FB}} \frac{m_B^*}{(k^2 + m_B^{*2})^{1/2}} k^2 dk, \quad (9)$$

$$n_B = (2J_B + 1) \frac{k_{FB}^3}{6\pi^2}, \quad (10)$$

where Fermi momentum is  $k_{FB}$ , spin is  $J_B$ , and isospin projection is  $I_{3B}$ . Effective mass and chemical potential of baryon  $B$  are  $m_B^* = m_B - g_{\sigma B}\sigma - g_{\sigma^*B}\sigma^*$  and  $\mu_B = (k_{FB}^2 + m_B^{*2})^{1/2} + g_{\omega B}\omega_0 + g_{\phi B}\phi_0 + I_{3B}g_{\rho B}\rho_{03}$ , respectively.

As the hadronic phase is charge neutral, the total charge density is

$$Q = \sum_B q_B n_B - n_e - n_\mu = 0 , \quad (11)$$

where  $n_B$  is the number density of baryon B,  $q_B$  is the electric charge and  $n_e$  and  $n_\mu$  are charge densities of electrons and muons respectively.

In compact star interior, hyperons maintain chemical equilibrium through weak processes. The generalised  $\beta$ -decay processes may be written in the form  $B_1 \rightarrow B_2 + l + \bar{\nu}_l$  and  $B_2 + l \rightarrow B_1 + \nu_l$  where  $B_1$  and  $B_2$  are baryons and l is a lepton. Therefore the generic equation for chemical equilibrium condition is

$$\mu_i = b_i \mu_n - q_i \mu_e , \quad (12)$$

where  $\mu_n$ ,  $\mu_e$  and  $\mu_i$  are respectively the chemical potentials of neutrons, electrons and i-th baryon and  $b_i$  and  $q_i$  are baryon and electric charge of i-th baryon respectively. The above equation implies that there are two independent chemical potentials  $\mu_n$  and  $\mu_e$  corresponding to two conserved charges i.e. baryon number and electric charge.

The total energy density is given by

$$\begin{aligned} \varepsilon = & \frac{1}{2} m_\sigma^2 \sigma^2 + \frac{1}{3} g_2 \sigma^3 + \frac{1}{4} g_3 \sigma^4 + \frac{1}{2} m_{\sigma^*}^2 \sigma^{*2} \\ & + \frac{1}{2} m_\omega^2 \omega_0^2 + \frac{1}{2} m_\phi^2 \phi_0^2 + \frac{1}{2} m_\rho^2 \rho_{03}^2 \\ & + \sum_B \frac{2J_B + 1}{2\pi^2} \int_0^{k_{FB}} (k^2 + m_B^{*2})^{1/2} k^2 dk \\ & + \sum_l \frac{1}{\pi^2} \int_0^{K_{Fl}} (k^2 + m_l^2)^{1/2} k^2 dk . \end{aligned} \quad (13)$$

And the pressure is

$$\begin{aligned} P = & -\frac{1}{2} m_\sigma^2 \sigma^2 - \frac{1}{3} g_2 \sigma^3 - \frac{1}{4} g_3 \sigma^4 \\ & - \frac{1}{2} m_{\sigma^*}^2 \sigma^{*2} + \frac{1}{2} m_\omega^2 \omega_0^2 + \frac{1}{2} m_\phi^2 \phi_0^2 + \frac{1}{2} m_\rho^2 \rho_{03}^2 \\ & + \frac{1}{3} \sum_B \frac{2J_B + 1}{2\pi^2} \int_0^{k_{FB}} \frac{k^4 dk}{(k^2 + m_B^{*2})^{1/2}} \\ & + \frac{1}{3} \sum_l \frac{1}{\pi^2} \int_0^{K_{Fl}} \frac{k^4 dk}{(k^2 + m_l^2)^{1/2}} . \end{aligned} \quad (14)$$

Bulk viscosity arises because pressure and density variations associated with the r-mode oscillation drive the system out of chemical equilibrium. Various microscopic reaction processes bring the system back to equilibrium. Weak interaction processes are most important

in this case. As we are concerned about bulk viscosity coefficient in young neutron stars where temperature is  $\sim 10^9 - 10^{10}$  K, it was shown by various authors [10, 11, 12, 13] that non-leptonic processes involving hyperons might lead to a high value for the bulk viscosity coefficient. Though there may be several processes contributing to the bulk viscosity, only those reactions which might provide an upper limit on the bulk viscosity would be of interest. The relevant non-leptonic processes are

$$n + p \rightleftharpoons p + \Lambda , \quad (15)$$

$$n + n \rightleftharpoons p + \Sigma , \quad (16)$$

$$n + n \rightleftharpoons n + \Lambda . \quad (17)$$

All these reactions involve variation of neutron number density ( $n_n$ ) due to density perturbation on the system. Therefore, we consider neutron fraction as a primary variable.

The real part of bulk viscosity coefficient is calculated in terms of relaxation times of microscopic processes [13, 26]

$$\zeta = \frac{P(\gamma_\infty - \gamma_0)\tau}{1 + (\omega\tau)^2} , \quad (18)$$

where  $P$  is the pressure,  $\tau$  is the net microscopic relaxation time and  $\gamma_\infty$  and  $\gamma_0$  are 'infinite' and 'zero' frequency adiabatic indices respectively. The factor

$$\gamma_\infty - \gamma_0 = -\frac{n_b^2}{P} \frac{\partial P}{\partial n_n} \frac{d\bar{x}_n}{dn_b} , \quad (19)$$

can be determined from the EoS. Here  $\bar{x}_n = \frac{n_n}{n_b}$  gives the neutron fraction in the equilibrium state and  $n_b = \sum_B n_B$  is the total baryon density. In the co-rotating frame, the angular velocity ( $\omega$ ) of (l,m) r-mode is related to angular velocity ( $\Omega$ ) of a rotating neutron star as  $\omega = \frac{2m}{l(l+1)}\Omega$  [1].

Here we consider the process in Eq. (15) because other processes may not contribute significantly to the calculation of bulk viscosity coefficient and are discussed later in details. The relaxation time ( $\tau$ ) for the process is given by [13]

$$\frac{1}{\tau} = \frac{(kT)^2}{192\pi^3} p_\Lambda < |M_\Lambda|^2 > \frac{\delta\mu}{n_b \delta x_n} , \quad (20)$$

where  $p_\Lambda$  is the Fermi momentum for  $\Lambda$  hyperons and  $< |M_\Lambda|^2 >$  is the angle averaged matrix element squared given by Ref.[10, 13]. Also, we have

$$\frac{\delta\mu}{n_b \delta x_n} = \alpha_{nn} - \alpha_{\Lambda n} - \alpha_{n\Lambda} + \alpha_{\Lambda\Lambda} , \quad (21)$$

where  $\delta x_n = x_n - \bar{x}_n$  is the departure of neutron fraction from its thermodynamic equilibrium value  $\bar{x}_n$  and  $\alpha_{ij} = \frac{\partial \mu_i}{\partial n_j}$  for  $n_k, k \neq j$  which is determined from the EoS. As soon as we know the relaxation time, we can calculate the bulk viscosity coefficient.

The bulk viscosity damping timescale ( $\tau_B$ ) due to the non-leptonic process involving hyperons is given by [10, 13]

$$\frac{1}{\tau_B} = -\frac{1}{2E} \frac{dE}{dt}, \quad (22)$$

where  $E$  is the energy of the perturbation as measured in the co-rotating frame of the fluid and is expressed as

$$E = \frac{1}{2} \alpha^2 \Omega^2 R^{-2} \int_0^R \epsilon(r) r^6 dr. \quad (23)$$

Here,  $\alpha$  is the dimensionless amplitude of the r-mode,  $R$  is the radius of the star and  $\epsilon(r)$  is the energy density profile. The derivative of the co-rotating frame energy with respect to time is

$$\frac{dE}{dt} = -4\pi \int_0^R \zeta(r) \langle |\vec{\nabla} \cdot \delta \vec{v}|^2 \rangle r^2 dr, \quad (24)$$

where the angle average of the square of the hydrodynamic expansion [27] is  $\langle |\vec{\nabla} \cdot \delta \vec{v}|^2 \rangle = \frac{(\alpha \Omega)^2}{690} \left(\frac{r}{R}\right)^6 (1 + 0.86 \left(\frac{r}{R}\right)^2) \left(\frac{\Omega^2}{\pi G \bar{\epsilon}}\right)^2$  and  $\bar{\epsilon}$  is the mean energy density of a non-rotating star. Equation (24) is the bulk viscosity contribution to the imaginary part of the frequency of the r-mode. Taking into account time scales for gravitational radiation ( $\tau_{GR}$ ) and modified Urca process ( $\tau_U$ ) involving only nucleons, we can define the overall r-mode time scale ( $\tau_r$ ) as

$$\frac{1}{\tau_r} = -\frac{1}{\tau_{GR}} + \frac{1}{\tau_B} + \frac{1}{\tau_U}. \quad (25)$$

Here  $\frac{1}{\tau_r}$  is the imaginary part of the frequency of the r-mode. The gravitational radiation timescale is given by [4]

$$\frac{1}{\tau_{GR}} = \frac{131072\pi}{164025} \Omega^6 \int_0^R \epsilon(r) r^6 dr. \quad (26)$$

The time scale due to modified Urca process ( $\tau_U$ ) involving only nucleons is calculated similarly as the hyperon bulk viscosity damping time scale but using the following expression for bulk viscosity coefficient for modified Urca process given by [4, 28]

$$\zeta_U = 6 \times 10^{-59} \epsilon^2 T^6 \omega^2. \quad (27)$$

Damping timescales are functions of angular velocity, neutron star mass and temperature. Therefore, solving  $\frac{1}{\tau_r} = 0$ , we calculate the critical angular velocity above which the r-mode is unstable whereas it is stable below the critical angular velocity.

### III. RESULTS AND DISCUSSION

In this calculation, we require the knowledge of coupling constants for baryons with  $\sigma$ ,  $\omega$ ,  $\rho$ ,  $\sigma^*$  and  $\phi$  mesons. Nucleon-meson coupling constants are obtained by reproducing nuclear matter saturation properties and taken from Ref. [29]. Here we consider the parameter set corresponding to the value of incompressibility of nuclear matter  $K = 240$  MeV. Nucleon-meson coupling constants are listed in Table I.

Hyperon-vector meson coupling constants are determined from SU(6) symmetry of the quark model [23, 30, 31]. The scalar  $\sigma$  meson coupling to hyperons is calculated from the potential depth of a hyperon (Y)

$$U_Y^N(n_0) = -g_{\sigma Y}\sigma + g_{\omega Y}\omega_0, \quad (28)$$

in normal nuclear matter. The potential depth of  $\Lambda$  hyperons in normal nuclear matter  $U_\Lambda^N(n_0) = -30$  MeV is obtained from the analysis of energy levels of  $\Lambda$  hypernuclei [30, 32]. Recent  $\Xi$ -hypernuclei data from various experiments [33, 34] give a relativistic potential of  $U_\Xi^N(n_0) = -18$  MeV. However, the analysis of  $\Sigma^-$  atomic data implies a strong isoscalar repulsion for  $\Sigma^-$  hyperons in nuclear matter [21]. Also, recent  $\Sigma$  hypernuclei data indicate a repulsive  $\Sigma$ -nucleus potential depth [35]. Therefore, we adopt a repulsive potential depth of 30 MeV for  $\Sigma$  hyperons [21].

The hyperon- $\sigma^*$  coupling constants are estimated by fitting them to a potential depth,  $U_Y^{(Y')}(n_0)$ , for a hyperon (Y) in a hyperon ( $Y'$ ) matter at normal nuclear matter density obtained from double  $\Lambda$  hypernuclei data [22, 23]. This is given by

$$U_\Xi^{(\Xi)}(n_0) = U_\Lambda^{(\Xi)}(n_0) = 2U_\Xi^{(\Lambda)}(n_0) = 2U_\Lambda^{(\Lambda)}(n_0) = -40. \quad (29)$$

Now we perform our calculation employing nucleon-meson and hyperon-meson coupling constants corresponding to  $K = 240$  MeV case. We find that before the appearance of hyperons, the  $\beta$ -equilibrated matter is composed of neutrons, protons, electrons and muons and their abundances increase with baryon density. Here, charge neutrality is maintained by protons, electrons and muons. Particle populations as a function of baryon density and without hyperon-hyperon interaction are displayed in Fig. 1. At  $2.6n_0$ ,  $\Lambda$  hyperons appear first in the system. It is observed that the density of  $\Lambda$  hyperon increases whereas the neutron density decreases with increasing baryon density for the growth of  $\Lambda$  hyperons occurs at the

expense of neutrons. Next  $\Xi^-$  hyperons are populated around  $3.0n_0$ . However,  $\Sigma$  hyperons do not appear in the system even at higher densities because of repulsive  $\Sigma$ -nuclear matter interaction. Further we note that threshold densities for the appearance of different hyperon species except  $\Xi^0$  hyperons are not changed appreciably due to hyperon-hyperon interaction and this is demonstrated in Fig. 2.

Equations of state (pressure versus energy density) for different compositions are shown in Fig. 3. The bold solid curve implies nucleons-only matter whereas the dashed and solid curves correspond to hyperon matter with and without interaction, respectively. The appearance of hyperons makes equations of state softer. On the other hand, the EoS with hyperon-hyperon interaction is initially softer compared with the case without the interaction, but it becomes stiffer later. This may be understood in the following way. Hyperon-hyperon interaction is mediated by  $\sigma^*$  and  $\phi$  mesons. The additional attraction of  $\sigma^*$  field makes the EoS softer. The repulsive contribution of  $\phi$  field becomes dominant at higher densities. There is a competition between these two effects. Consequently, the EoS changes over from softer to stiffer at higher energy densities.

Now we calculate the bulk viscosity coefficient using the EoS including hyperon-hyperon interaction. Already, we have noted that  $\Lambda$  hyperons are populated first in the system and heavier hyperons appear at higher densities. Therefore, we are interested in non-leptonic processes, Eqs. (15) and (17), involving  $\Lambda$  hyperons. However, it was noted that transition rate for the non-leptonic process in Eq. (17) was one order of magnitude greater than that of the process in Eq. (15) and led to a lower relaxation time in the former case [12]. Therefore, we only consider the process in Eq. (15). In this calculation, partial derivatives of pressure and chemical potentials with respect to particle number density are determined with the help of the EoS. In Fig. 4, the difference of fast and slow adiabatic indices ( $\gamma_\infty - \gamma_0$ ) is plotted with normalised baryon density. The dashed curve represents the case with hyperon-hyperon interaction whereas the solid curve indicates the case without the interaction. The dashed curve rises to a maximum value and then drops below the solid curve. This can be attributed to the interplay of  $\sigma^*$  and  $\phi$  fields and the crossover from a softer to a stiffer EoS.

Next we compute the relaxation time as given by Eq. (20) for the process in Eq. (15). Effective masses, Fermi momenta, chemical potentials of baryons and partial derivatives entering into the expression of the relaxation time are obtained from the EoS. In the calculation of matrix element, we use the values of axial-vector coupling constants  $g_{np} = -1.27$  and  $g_{p\Lambda} =$

-0.72 obtained from  $\beta$ -decay of baryons at rest. We exhibit the relaxation time as a function of normalised baryon density in Fig. 5. The temperature is set to  $10^{10}$  K in this case. The dashed and solid curves denote cases with and without hyperon-hyperon interaction, respectively. We observe that the effect of the interaction on the relaxation time is not significant. Further, the behaviour of relaxation time with temperature for hyperon-hyperon interaction case is shown in Fig. 6. The relaxation time increases as the temperature is decreased. The effect of temperature on the relaxation time is substantial.

The hyperon bulk viscosity coefficient is plotted with normalised baryon density for a temperature  $10^{10}$  K in Fig. 7. For this calculation we obtain angular velocities ( $\Omega$ ) at different central densities corresponding to a sequence of neutron stars using the rotating star model [36, 37] and equations of state with and without hyperon-hyperon interaction. We note that the factor  $\omega\tau$  is much much less than 1 over the range of baryon densities that we have shown here and is neglected in the bulk viscosity coefficient given by Eq. (18). The bulk viscosity coefficient in hyperon-hyperon interaction case represented by the dashed curve becomes smaller than that without the interaction denoted by the solid curve in the density regime which might occur in maximum mass neutron stars. The effect of the interaction enters into the bulk viscosity coefficient through the pressure term and adiabatic indices. The bulk viscosity coefficient increases appreciably with decreasing temperature as it is evident from Fig. 8. The large value of  $\zeta$  at  $10^9$  K indicates that the viscous damping might be important in suppressing r-mode instability in neutron stars. It is to be noted here that we have neglected  $\Lambda$ -hyperon superfluidity in this calculation. Earlier calculations of bulk viscosity with hyperons involved hyperon superfluidity [10, 13]. However, it has been reported that superfluid gaps for hyperons would be very small [38, 39].

Now we discuss the effect of the EoS including hyperon-hyperon interaction on the stability of r-mode. This mode becomes stable when the gravitational radiation timescale is greater than the damping timescales due to hyperon bulk viscosity as well as modified Urca bulk viscosity. The calculation of bulk viscosity timescales as given by Eqs. (22)-(24) needs the structure of a neutron star and its energy density profile. We have calculated the sequences of non-rotating neutron stars using Tolman-Oppenheimer-Volkoff equations with and without hyperon-hyperon interaction. The maximum neutron star masses with and without hyperon-hyperon interaction are  $1.64 M_{solar}$  and  $1.69 M_{solar}$  corresponding to central baryon densities  $7.1$  and  $6.9 n_0$ , respectively. Similarly, we have computed sequences

of rotating stars with and without hyperon-hyperon interaction using rotating neutron star model of Stergioulas [6, 36, 37]. In this case, maximum masses of rotating neutron stars with and without hyperon-hyperon interaction are  $1.95 M_{solar}$  and  $2.00 M_{solar}$  corresponding to central baryon densities  $5.4$  and  $5.7 n_0$  respectively.

Next we perform the calculation of damping timescale due to hyperon bulk viscosity with and without hyperon-hyperon interaction for rotating neutron stars of mass  $1.6 M_{solar}$ . This requires the knowledge of energy density profiles in rotating neutron stars. Earlier investigations adopted slowly rotating neutron stars and used the energy density profiles of non-rotating neutron stars [13]. Recently, Nayyar and Owen [10] incorporated the effects of rotation in the calculation of critical angular velocity using Hartle's slow rotation approximation. Here we also include the effects of rotation on damping time scale using energy density profiles of rotating neutron stars. A rotating neutron star has less central energy density than that of its non-rotating counterpart having the same gravitational mass because of the contribution from centrifugal force. Therefore, hyperon population will be sensitive to the rotation. Here we are dealing with a situation where the young neutron star is rotating very fast and radiating gravitational waves giving rise to the r-mode instability in it. As the neutron star emits gravitational radiation it spins down. Consequently, the central density in it increases. When the baryon density in the interior is such that hyperon thresholds are reached, hyperons will be produced abundantly. In this calculation, we consider  $1.6 M_{solar}$  mass neutron stars with and without hyperon-hyperon interaction having central baryon densities  $3.9$  and  $3.6 n_0$  which are much above the threshold for  $\Lambda$  hyperons and rotating at angular velocities  $\Omega_{rot} = 2952 s^{-1}$  and  $3100 s^{-1}$  respectively. We calculate the hyperon bulk viscosity damping time scales using the energy density profiles of those stars. Their energy density profiles with and without hyperon-hyperon interaction are displayed in Fig. 9. The dashed curve including the interaction has larger energy densities than the case without the interaction. It is to be noted that the Keplerian angular velocities of neutron stars of mass  $1.6 M_{solar}$  with and without the interaction are  $5600 s^{-1}$  and corresponding central baryon densities are below the hyperon thresholds. The angular velocity for  $l=m=2$  r-mode for a neutron star rotating with angular velocity ( $\Omega$ ) is given by  $\omega = \frac{2}{3}\Omega$ . In this calculation we obtain a set of values for  $\omega$  corresponding to  $\Omega$  ranging from  $0$  to  $\Omega_{rot}$ . Also, we express hyperon bulk viscosity  $\zeta$  as a function of  $r$  using the knowledge of baryon density profiles. All these inputs are now used to calculate the damping timescale. Similarly, we calculate

the damping timescale due to modified Urca process for nucleons using the expression for the bulk viscosity coefficient Eq. (27). However, the bulk viscosity due to leptonic processes is several orders of magnitude lower than that of non-leptonic processes and has small effect on the damping of the mode. It is to be noted here that the effect of direct Urca process involving hyperons on bulk viscosity was investigated and it was found to have a small effect on the damping of the r-mode [13]. As the gravitational radiation drives the r-mode unstable, it comes with a negative sign in Eq. (25). It is worth mentioning here that the energy density profiles of rotating stars used in this calculation do not differ much from their non-rotating counterparts.

Now we determine critical angular velocities ( $\Omega_C$ ) as a function of temperature for a neutron star of mass  $1.6 M_{solar}$  by solving  $\frac{1}{\tau_r} = 0$  as given by Eq. (25). The critical angular velocity is plotted with temperature in Fig. 10 for cases with (dashed curve) and without (solid curve) hyperon-hyperon interaction. We find that two curves do differ a little bit at and above  $5 \times 10^9$  K. This implies that gravitational radiation dominates in this region making the r-modes unstable. However, below this temperature damping timescales due to hyperon bulk viscosity starts dominating. The hyperon-hyperon interaction suppresses the instability more effectively below  $5 \times 10^9$  K. Consequently, the instability window shrinks.

#### IV. SUMMARY AND CONCLUSIONS

We have studied the effect of exotic matter, in particular, hyperon matter including hyperon-hyperon interaction on bulk viscosity. Here we have constructed equations of state within the framework of a relativistic field theoretical model. As large number of hyperons may be produced in dense matter, hyperon-hyperon interaction becomes important and have been included in our calculation. This interaction is mediated by two strange mesons. Here, we use recent hypernuclei data which give rise to attractive potential depths for  $\Lambda$  and  $\Xi$  hyperons and a repulsive potential depth for  $\Sigma$  hyperons in normal nuclear matter. Also, we exploit the knowledge of double  $\Lambda$  hypernuclei data to find the strength of hyperon- $\sigma^*$  meson coupling constant. Using these potential depths, we find that  $\Lambda$  hyperons appears first in the system followed by  $\Xi^-$  and  $\Xi^0$  hyperons. However,  $\Sigma$  hyperons do not appear because of the repulsive potential. Hyperon-hyperon interaction makes the EoS softer resulting in a smaller maximum mass neutron star than that without the interaction. Next we have computed

the bulk viscosity coefficient due to the non-leptonic weak process  $n + p \rightleftharpoons p + \Lambda$  and its influence on r-mode stability. We have used energy density profiles for rotating neutron stars to take into account the effects of rotation on hyperon populations. It is found that the gravitational radiation driven r-mode instability is more effectively suppressed due to the bulk viscosity coefficient in hyperon-hyperon interaction case compared with the situation without the interaction.

Besides hyperon matter, there might be other forms of matter such as Bose-Einstein condensates of antikaons and quarks. It was shown in earlier calculations that Bose-Einstein condensation of antikaons might appear around  $2-3n_0$  and delay the appearance of hyperons [40]. So far, there is no calculation of bulk viscosity in the antikaon condensed phase due to non-leptonic processes and how it competes with hyperon bulk viscosity coefficient. This problem is being investigated by us and will be reported in a future publication.

- 
- [1] N. Andersson, *Class. Quant. Grav.* **20**, R105 (2003).
  - [2] N. Andersson, *Astrophys J.* **502**, 708 (1998).
  - [3] J. L. Friedman and S. M. Morsink, *Astrophys J.* **502**, 714 (1998).
  - [4] L. Lindblom, B.J. Owen and S. M. Morsink, *Phys. Rev. Lett.* **80**, 4843 (1998).
  - [5] N. Andersson, K. D. Kokkotas and B. F. Schutz, *Astrophys J.* **510**, 846 (1999).
  - [6] N. Stergioulas, *Liv. Rev. Rel.* **6**, 3 (2003).
  - [7] D. Chakrabarty, *ASP Conference Series: Binary Radio Pulsars*, Eds. F. Rasio and I. Stairs, **328**, 279 (2005).
  - [8] D. Chakrabarty et al., *Nature* **424**, 42 (2003).
  - [9] J.W.T. Hessels et al., *astro-ph/0601337*.
  - [10] M. Nayyar and B.J. Owen, *Phys. Rev. D* **73**, 084001 (2006).
  - [11] P.B. Jones, *Phys. Rev. Lett.* **86**, 1384 (2001).
  - [12] P.B. Jones, *Phys. Rev. D* **64**, 084003 (2001).
  - [13] L. Lindblom and B.J. Owen, *Phys. Rev. D* **65**, 063006 (2002).
  - [14] E.N.E. van Dalen and A.E.L. Dieperink, *Phys. Rev. C* **69**, 025802 (2004).
  - [15] A. Drago, A. Lavagno and G. Pagliara, *Phys. Rev. D* **71**, 103004 (2005).
  - [16] J. Madsen, *Phys. Rev. D* **46**, 3290 (1992).

- [17] J. Madsen, Phys. Rev. Lett. **85**, 10 (2000).
- [18] D. Gondek-Rosinska, E. Gourgoulhon and P. Haensel, Astron. Astrophys. **412**, 777 (2003).
- [19] S. Balberg and A. Gal, Nucl. Phys. **A625**, 435 (1997).
- [20] D. Bandyopadhyay, nucl-th/**0512100**.
- [21] E. Friedman, A. Gal and C. J. Batty, Nucl. Phys. **A579**, 518 (1994); C. J. Batty, E. Friedman and A. Gal, Phys. Rep. **287**, 385 (1997).
- [22] J. Schaffner, C.B. Dover, A. Gal, C. Greiner and H. Stöcker, Phys. Rev. Lett. **71**, 1328 (1993).
- [23] J. Schaffner and I.N. Mishustin, Phys. Rev. C **53**, 1416 (1996).
- [24] J. Boguta and A. R. Bodmer, Nucl. Phys. **A292**, 413 (1977).
- [25] B. D. Serot and J. D. Walecka, Adv. Nucl. Phys. **16**, 1 (1986).
- [26] L.D. Landau and E.M. Lifshitz, Fluid Mechanics, 2nd ed. (Butterworth-Heinemann, Oxford, 1999).
- [27] L. Lindblom, G. Mendell and B.J. Owen, Phys. Rev. D **60**, 064006 (1999).
- [28] R.F. Sawyer, Phys. Rev. D **39**, 3804 (1989).
- [29] N. K. Glendenning and S. A. Moszkowski, Phys. Rev. Lett. **67**, 2414 (1991).
- [30] C. B. Dover and A. Gal, Prog. Part. Nucl. Phys. **12**, 171 (1984).
- [31] J. Schaffner, C.B. Dover, A. Gal, D. J. Millener, C. Greiner and H. Stöcker, Ann. Phys. (N.Y.) **235**, 35 (1994).
- [32] R. E. Chrien and C. B. Dover, Annu. Rev. Nucl. Part. Sci. **39**, 113 (1989).
- [33] T. Fukuda et al., Phys. Rev. C **58**, 1306 (1998).
- [34] P. Khaustov et al., Phys. Rev. C **61**, 054603 (2000).
- [35] S. Bart et al., Phys. Rev. Lett. **83**, 5238 (1999).
- [36] N. Stergioulas and J. L. Friedman, Astrophys. J. **444**, 306 (1995).
- [37] We adopt the RNS code of Stergioulas (Ref. [36]) to calculate the structure of rotating stars and their Kepler frequencies.
- [38] H. Takahashi et al., Phys. Rev. Lett. **87**, 212502 (2001).
- [39] S. Tsuruta, astro-ph/**0602138**.
- [40] S. Banik and D. Bandyopadhyay, Phys. Rev. C **64**, 055805 (2001).

TABLE I: The nucleon-meson coupling constants in the GM1 set are taken from Ref. [29]. The coupling constants are obtained by reproducing the nuclear matter properties of binding energy  $E/B = -16.3$  MeV, baryon density  $n_0 = 0.153$  fm $^{-3}$ , asymmetry energy coefficient  $a_{\text{asy}} = 32.5$  MeV along with incompressibility  $K = 240$  MeV, and effective nucleon mass  $m_N^*/m_N = 0.78$ . The hadronic masses are  $m_N = 938$  MeV,  $m_\sigma = 550$  MeV,  $m_\omega = 783$  MeV, and  $m_\rho = 770$  MeV. All coupling constants are dimensionless, except  $g_2$  which is in fm $^{-1}$ .

K (MeV)	$g_{\sigma N}$	$g_{\omega N}$	$g_{\rho N}$	$g_2$	$g_3$
240	8.7822	8.7122	8.5416	27.8812	-14.3970

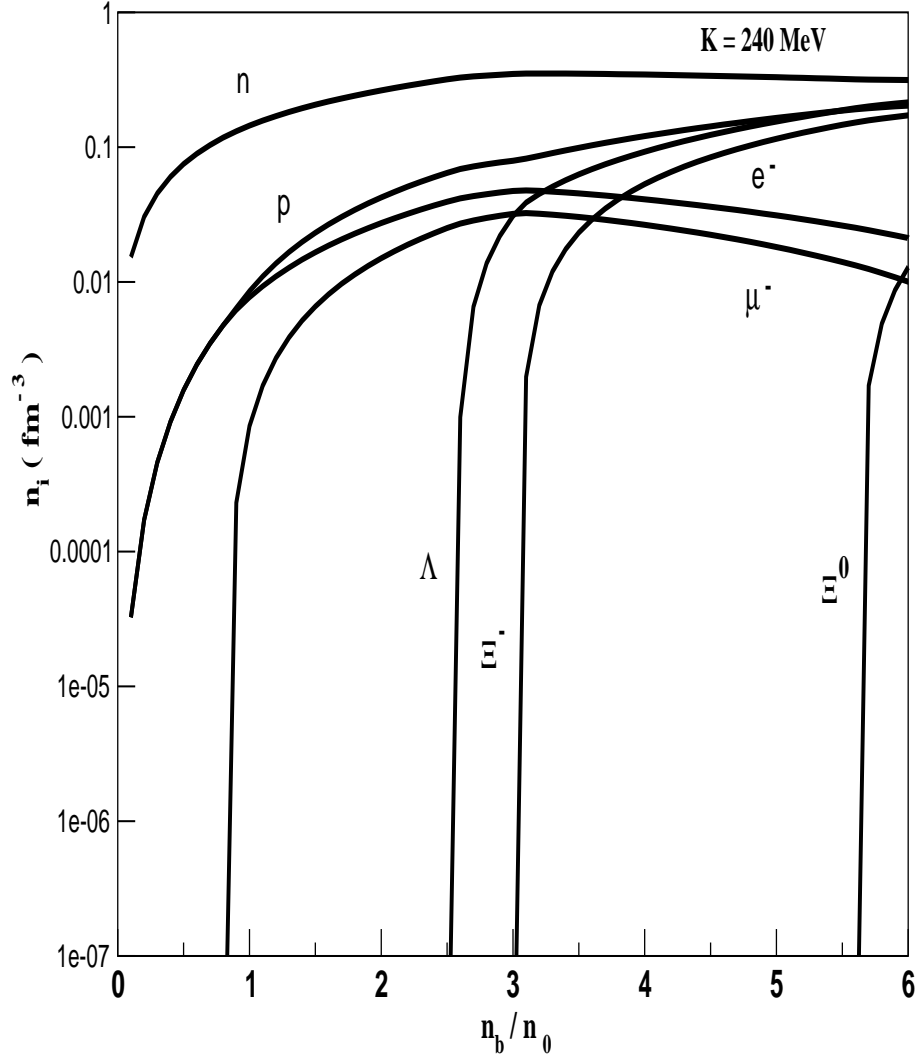


Fig. 1. Particles abundances are plotted with normalised baryon density for the case without hyperon-hyperon interaction.

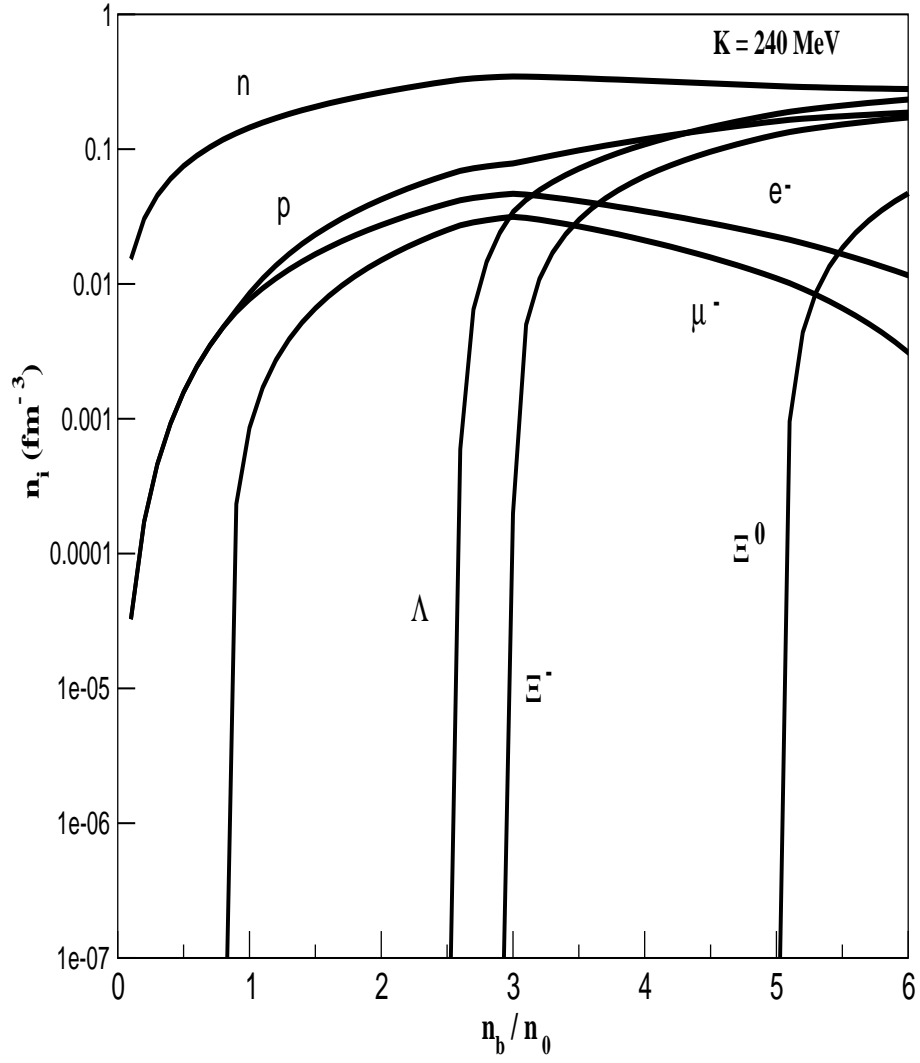


Fig. 2. Same as in Fig. 1 but for hyperon-hyperon interaction case.

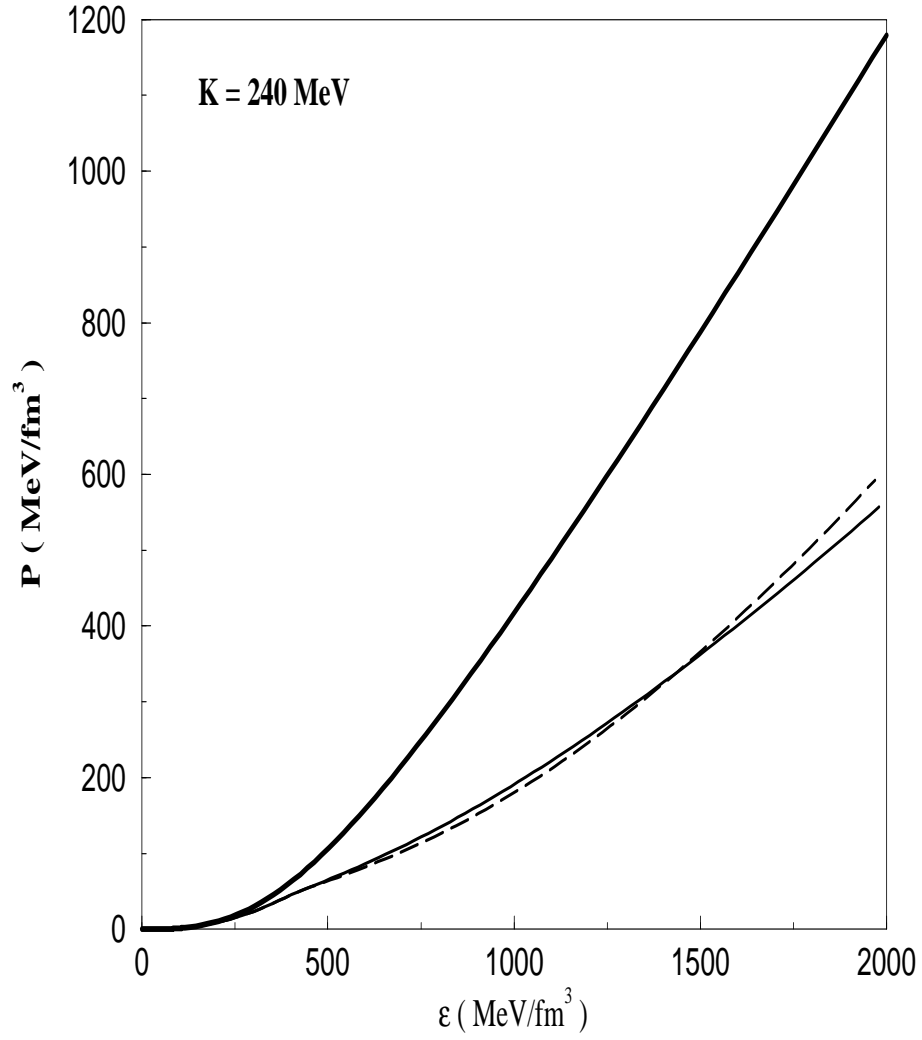


Fig. 3. The equation of state, pressure  $P$  vs energy density  $\epsilon$ , for nucleons-only matter (bold solid curve), hyperon matter with (dashed curve) and without (solid curve) hyperon-hyperon interaction are shown here.

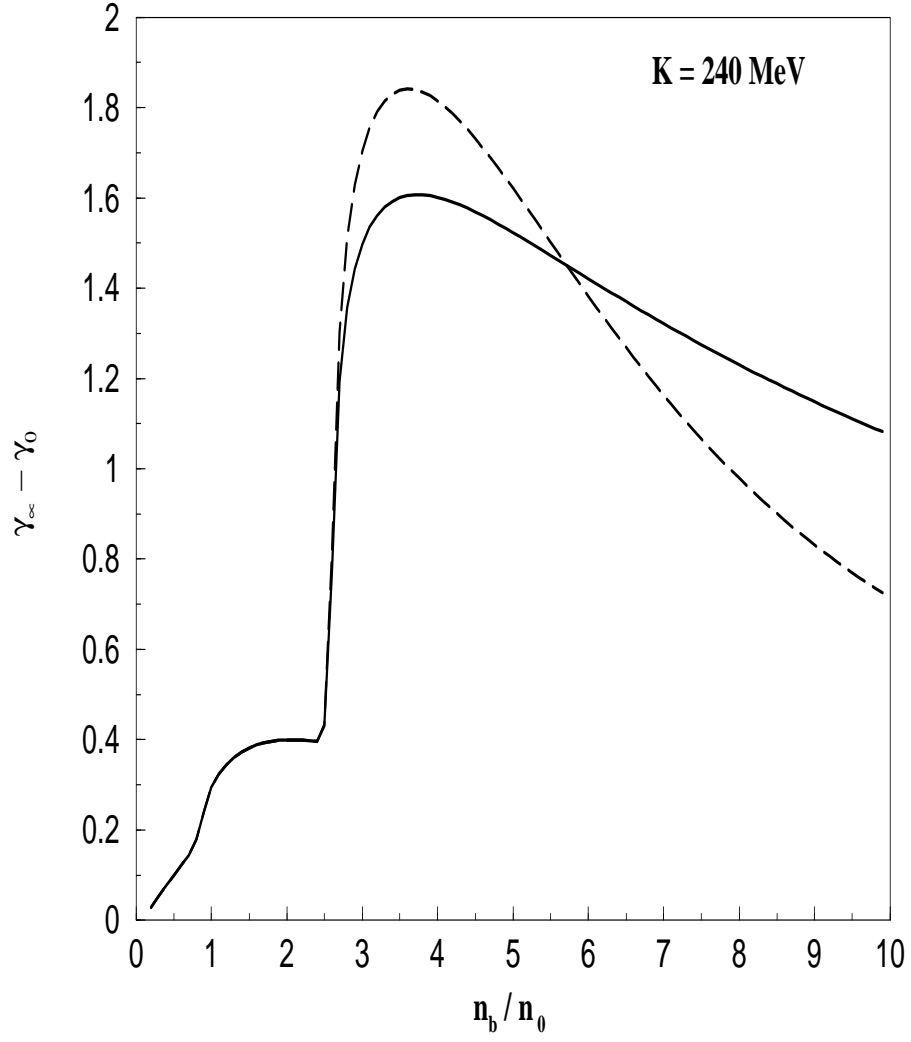


Fig. 4. The difference of adiabatic indices,  $\gamma_\infty - \gamma_0$ , is shown as a function of normalised baryon density with (dashed) and without (solid curve) hyperon-hyperon interaction.

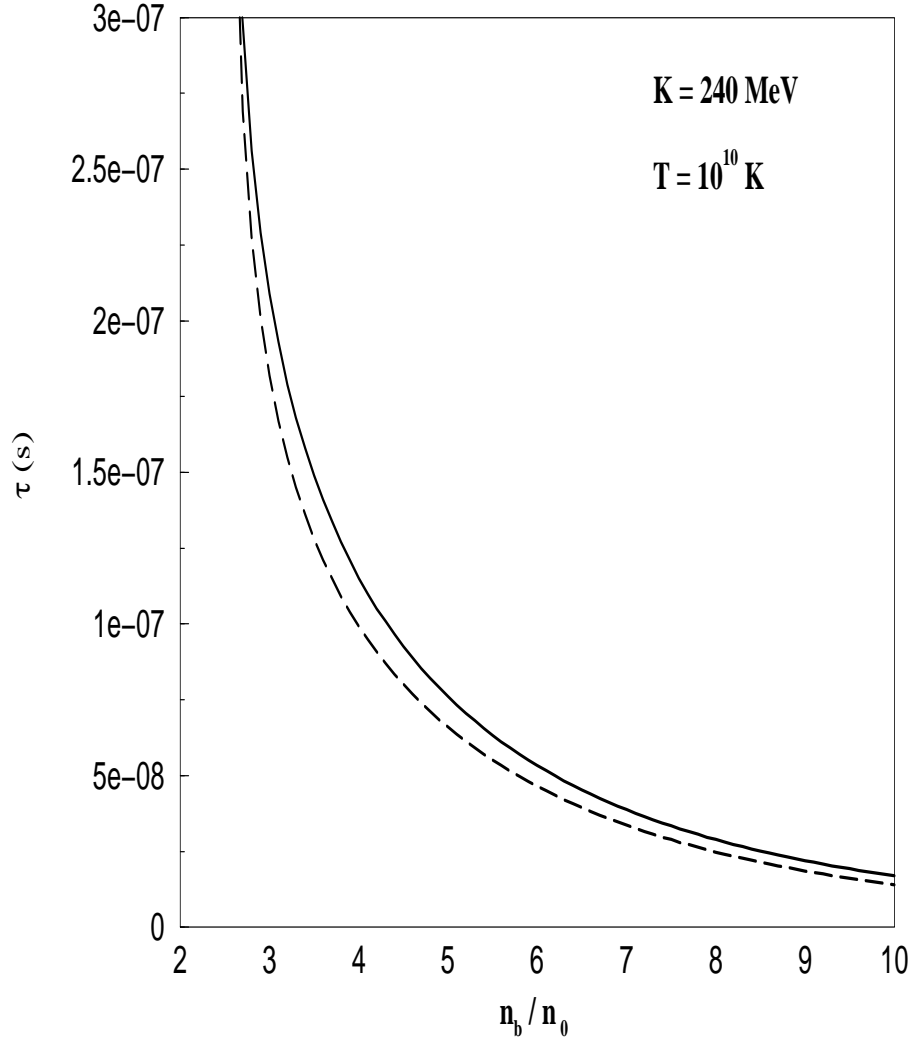


Fig. 5. Relaxation time is plotted with normalised baryon density for the non-leptonic process in Eq. (15) at a temperature  $10^{10}$  K for hyperon matter with (dashed curve) and without (solid curve) hyperon-hyperon interaction.

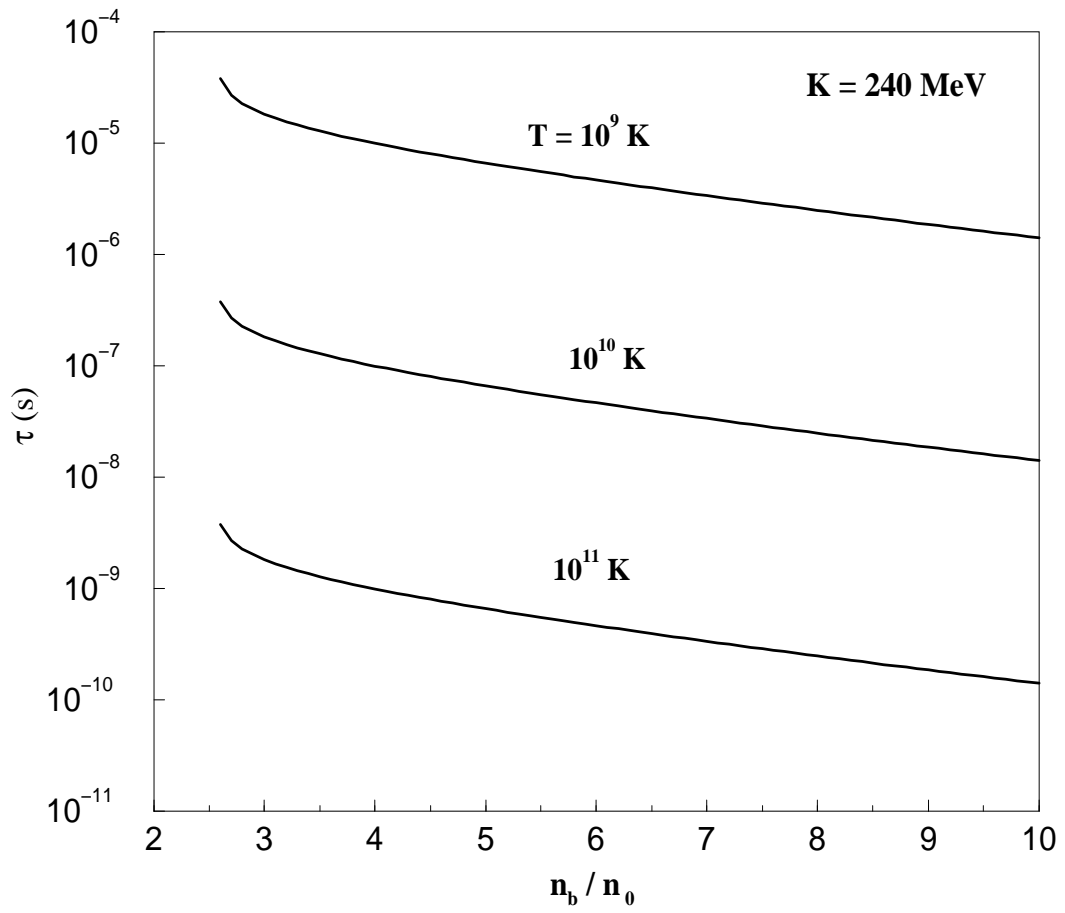


Fig. 6. Same as in Fig. 5 but for different temperatures and with hyperon-hyperon interaction.

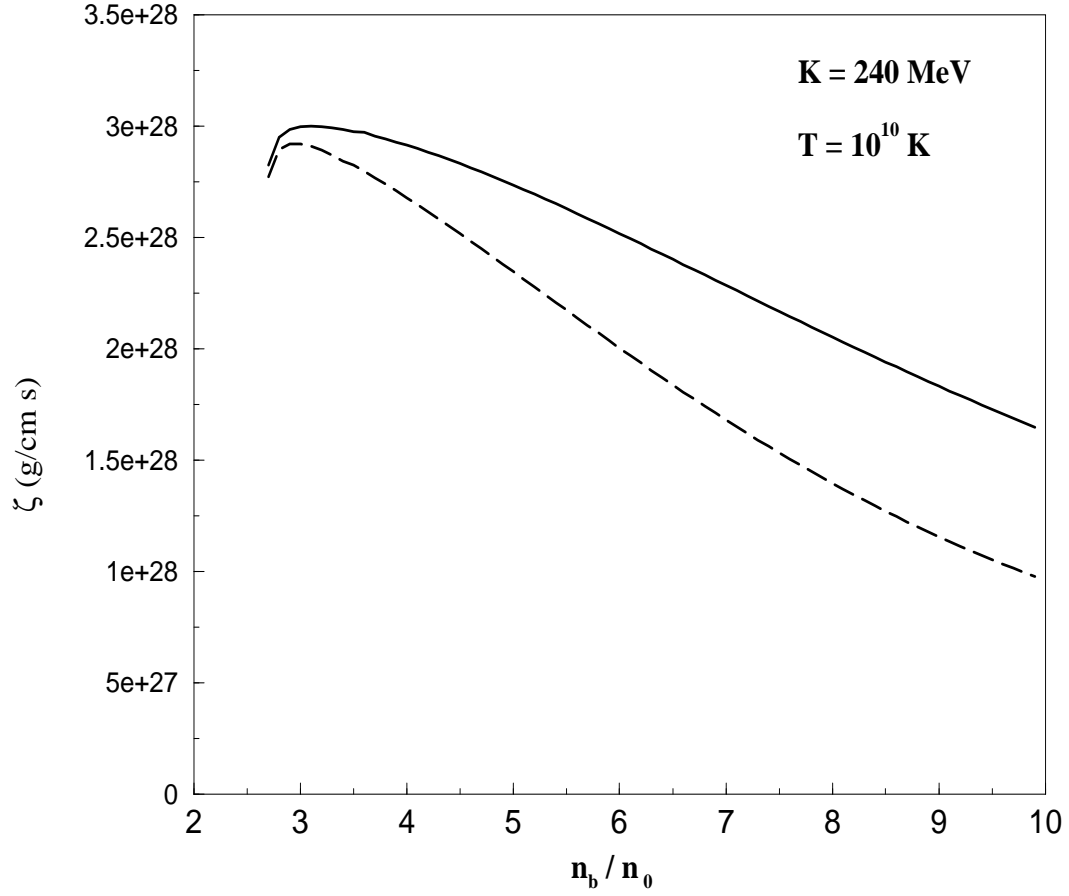


Fig. 7. Bulk viscosity coefficient is exhibited as a function of normalised baryon density for the process in Eq. (15) at a temperature  $10^{10}$  K for hyperon matter with (dashed curve) and without (solid curve) hyperon-hyperon interaction.

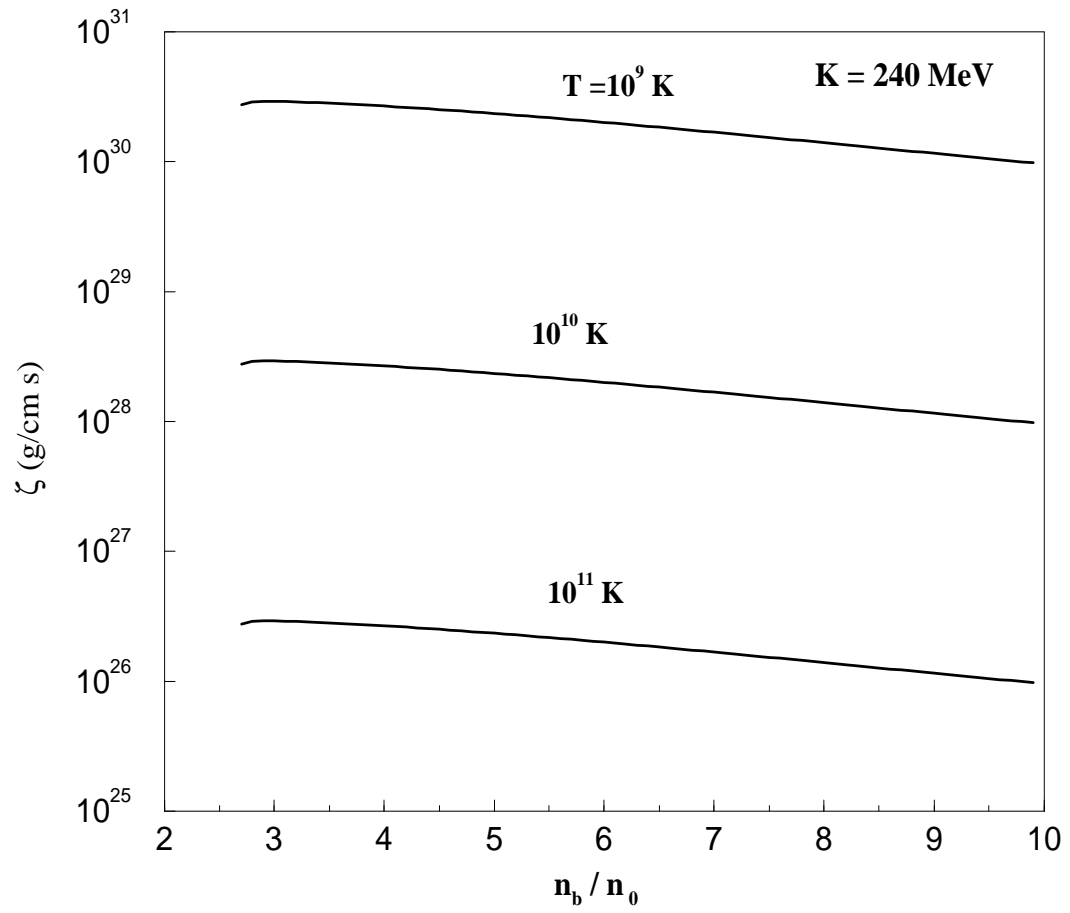


Fig. 8. Same as in Fig. 5 but for different temperatures and hyperon-hyperon interaction.

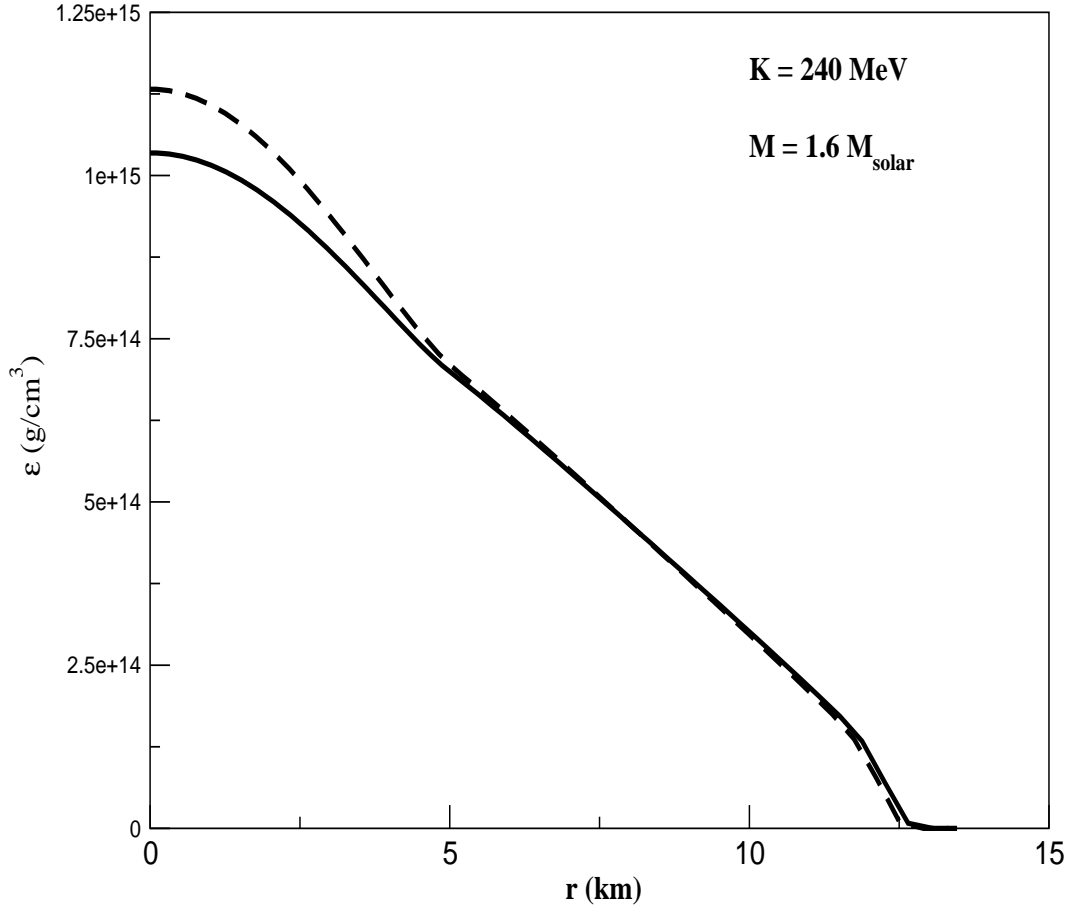


Fig. 9. Energy density profile is shown with radial distance for rotating neutron stars of mass  $1.6 M_{\text{solar}}$  with (dashed curve) and without (solid curve) hyperon-hyperon interaction.

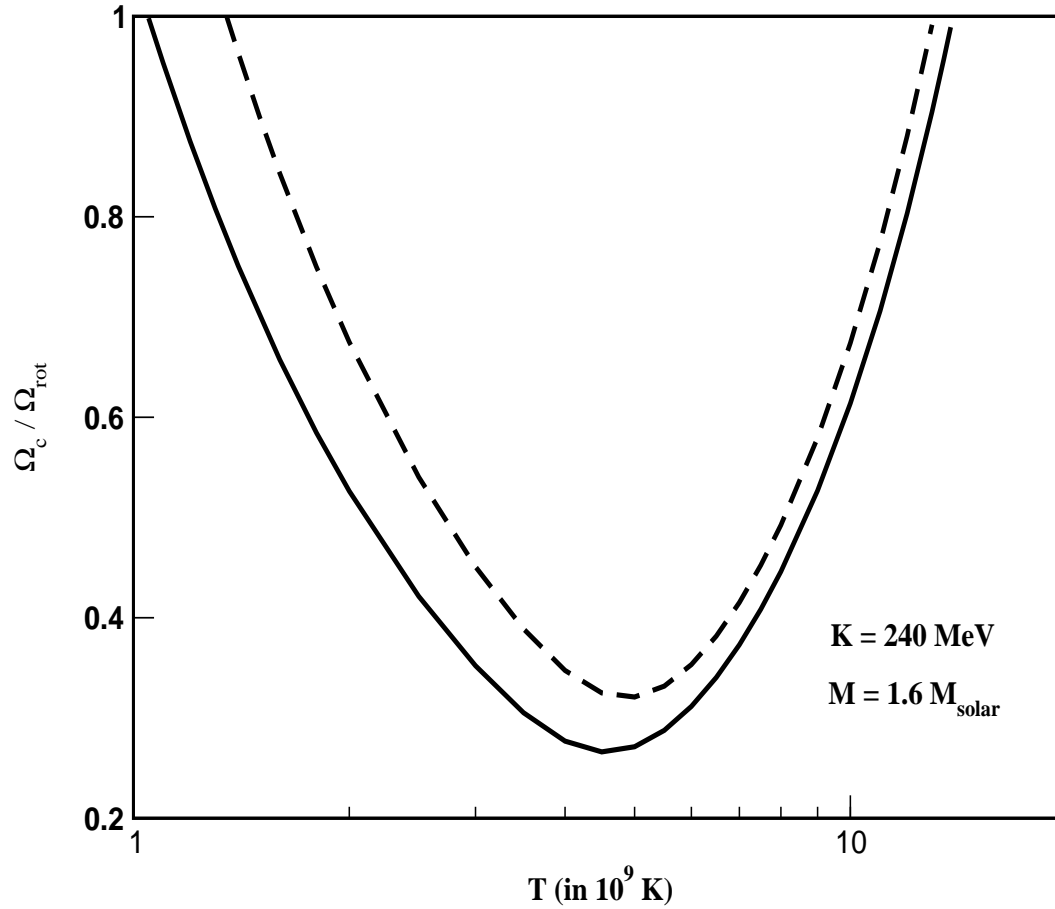


Fig. 10. Critical angular velocities for  $1.6 M_{solar}$  neutron star are plotted as a function of temperature with (dashed curve) and without (solid curve) hyperon-hyperon interaction.